AFRL-RD-PS
TP-2010-1025

AFRL-RD-PS
TP-2010-1025

AN EXPERIMENTAL STUDY SHOWING THE EFFECTS ON A STANDARD PI CONTROLLER USING A SEGMENTED MEMS DM ACTING AS A MOD (λ) DEVICE: POSTPRINT

Julie Smith, et al.

Air Force Research Laboratory
3500 Aberdeen Ave SE
Kirtland AFB, NM 87117

01 July 2010

Technical Paper

APPROVED FOR PUBLIC RELEASE; DISTRIBUTION IS UNLIMITED.

AIR FORCE RESEARCH LABORATORY
Directed Energy Directorate
3550 Aberdeen Ave SE
AIR FORCE MATERIEL COMMAND
KIRTLAND AIR FORCE BASE, NM 87117-5776

REPORT DOCUMENTATION PAGE

Form Approved
OMB No. 0704-0188

1. REPORT DATE *(DD-MM-YYYY)* 01-06-2010	**2. REPORT TYPE** Technical Paper	**3. DATES COVERED** *(From - To)* Oct 1, 2009- Jun 1, 2010

4. TITLE AND SUBTITLE An Experimental Study Showing the Effects on a Standard PI Controller Using a Segmented MEMS DM Acting as a (λ) Device: Postprint	**5a. CONTRACT NUMBER** In House DF702204
	5b. GRANT NUMBER
	5c. PROGRAM ELEMENT NUMBER
6. AUTHOR(S) Julie C. Smith, *James Brown, Darryl J. Sanchez, *Denis W. Oesch, Patrick Kelly, Katia Shtyrova, Carylon M. Tewksbury-Christle	**5d. PROJECT NUMBER**
	5e. TASK NUMBER
	5f. WORK UNIT NUMBER
7. PERFORMING ORGANIZATION NAME(S) AND ADDRESS(ES) Air Force Research Laboratory, 3500 Aberdeen Ave SE, Kirtland AFB, NM 87117 *Science Applications International, 6109 Airpark Road Southeast, Albuquerque, NM 87106	**8. PERFORMING ORGANIZATION REPORT NUMBER**
9. SPONSORING / MONITORING AGENCY NAME(S) AND ADDRESS(ES) Air Force Research Laboratory 3500 Aberdeen Ave Kirtland AFB, NM 87116	**10. SPONSOR/MONITOR'S ACRONYM(S)** AFRL/RDS
	11. SPONSOR/MONITOR'S REPORT NUMBER(S) AFRL-RD-PS-TP-2010-1025

12. DISTRIBUTION / AVAILABILITY STATEMENT

Approved for Public Release

13. SUPPLEMENTARY NOTES

Accepted for publication in the SPIE annual conference; August 4, 2010; San Diego, CA. 377ABW-2010-1135, July 13, 2010.
"GOVERNMENT PURPOSE RIGHTS"

14. ABSTRACT

The ASALT lab has been investigating the use of a segmented MEMS DM in adaptive optics systems. One of the anticipated benefits of a segmented device is that in monochromatic light the throw is essentially infinite due to the modulo 2π nature of the device. Earlier work demonstrated how this modulo 2π behavior interacts unexpectedly with a standard proportional integral controller. Here we present experimental data on this effect to include the testbed on which the data was taken and the methodology used to measure the effect.

15. SUBJECT TERMS

Deformable Mirror, MEMS, Adaptive Optics, Control Law

16. SECURITY CLASSIFICATION OF:			**17. LIMITATION OF ABSTRACT**	**18. NUMBER OF PAGES**	**19a. NAME OF RESPONSIBLE PERSON**
					Patrick Kelly
a. REPORT Unclassified	**b. ABSTRACT** Unclassified	**c. THIS PAGE** Unclassified	SAR	16	**19b. TELEPHONE NUMBER** *(include area code)* 505-846-2094

Standard Form 298 (Rev. 8-98)
Prescribed by ANSI Std. 239.18

This page is intentionally left blank.

An Experimental Study Showing the Effects on a Standard PI Controller Using a Segmented MEMS DM Acting as a Mod(λ)Device

Julie C. Smith[1], James Brown[2] Darryl J. Sanchez[1], Denis W. Oesch[2], Patrick Kelly[1] Katia Shtyrkova[1] Carolyn M. Tewksbury-Christle[1]

[1]*Starfire Optical Range, AFRL/RDS, Kirtland AFB, Albuquerque, NM. 87117, USA*

[2]*Science Applications International Corporation, Albuquerque, New Mexico, USA*

Abstract: The ASALT lab has been investigating the use of a segmented MEMS DM in adaptive optics systems. One of the anticipated benefits of a segmented device is that in monochromatic light the throw is essentially infinite due to the modulo 2π nature of the device. Earlier work demonstrated how this modulo 2π behavior interacts unexpectedly with a standard proportional integral controller. Here we present experimental data on this effect to include the testbed on which the data was taken and the methodology used to measure the effect. *Keywords: Deformable Mirror, MEMS, Adaptive Optics, Control Law*

1. INTRODUCTION AND BACKGROUND

For centuries astronomers have been plagued by effects of the atmosphere on their ground based images. Images formed on the focal plane of a telescope suffer from phase distortion and an overall tilt on wavefronts caused by atmospheric turbulence. This causes aberrated images to form at the focal plane, decreasing overall performance of the imaging system. The advent of adaptive optics has greatly enhanced the performance and quality of imaging systems, especially in the astronomical community. Many astronomical discoveries would not have been possible without the use of adaptive optics.

Ground based telescopes using adaptive optics systems have the capability of achieving diffraction-limited imaging and therefore can produce high quality science. An AO system consists of three major components: a wavefront sensor (WFS) to detect the optical disturbance, a deformable mirror (DM) to correct for the optical disturbance, and a control computer to monitor the sensor information.[1] These systems work to remove higher order distortions to stabilize the position of the astronomical images by removing the overall tilt.[2] AO systems simultaneously relay the image to the science camera while removing the higher order aberrations with the DM and tilt aberrations with a fast steering mirror (FSM) leaving only minor amounts of residual error in the wave front .[2] Figure 1 shows a simplified schematic diagram of an adaptive optics system consisting of a FSM, DM, WFS, and controlling computer.

Conventional AO systems use a continuous face sheet DM, i.e. a DM with N number of actuators with finite throw. These DM's are known to perform very well in moderate to mild turbulence. Here we inves-

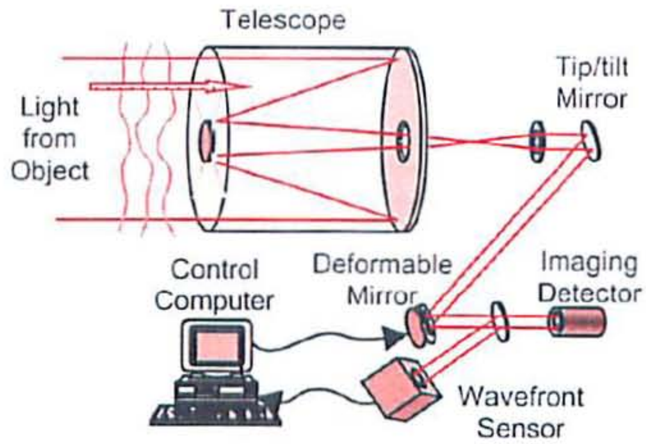

Fig. 1. *Diagram of a typical AO system*

tigate a smaller, segmented Micro-Electrical-Mechanical-System (MEMS) DM. MEMS is the integration of mechanical elements, sensors, actuators and electronics on a common silicon substrate through microfabrication technology. MEMS brings together silicon-based mircoelectronics with micromachining technology, making possible the realization of complete systems on a chip. The ASALT lab at Starfire Optical Range has been investigating the performance of a MEMS segmented DM in various turbulent regimes. We have successfully characterized the performance of this device and compared performance to that of a continuous face sheet DM used in conventional adaptive optics[3,4,5] and we have now turned our attention to the impact a segmented DM has on conventional control law.

commas should be in superscript

2. PROBLEM FORMULATION–CONTROL LAW

This research focuses on the AO control law. Conventional control law uses what is known as a proportional-integral (PI) controller, to monitor information from the wavefront sensors and to determine what commands should be sent to the DM. We implemented this standard controller with the MEMS DM and found the performance degraded greatly compared to a continuous face sheet DM ran with the same controller.[4] Initial data showed the reason for this degradation was due to the real time reconstructor (RTR). In the ASALT lab the phase information is measured by a self-referencing interferometer (SRI) which captures $mod(2\pi)$ phase. This phase information needs to be converted to a functional form that the DM can use; this process is called reconstructing the wavefront and is accomplished by the RTR. The RTR best fits the measured phase with a continuous 2-D function, calculates tilt and piston and subtracts both of those and a reference map to produce the residual phase. The output of the RTR goes to the DM controller where the mirror commands are calculated using,

$$y_k = A * y_{k-1} + B * \phi_r \tag{1}$$

where y_k is the DM command at time step k, ϕ_r is the residual phase, A is the 'leak', and B is the servo gain. The A gain is also known as an integrator. The integrator induces memory of the previous aberrations in the system, while the B gain is the resulting correction needed.

For conventional AO systems using a continuous face sheet DM, a least squares estimation is generally used to produce an estimate of the residual phase, and is currently the method of choice used in most

RTR's. Since the output of the SRI is in $mod(2\pi)$ space, the RTR must "unwrap" the phase before sending commands to the DM. Since the MEMS is a $mod(\lambda)$ device this unwrapping of the phase is unnecessary. When used on the MEMS DM, this RTR causes the actuator to "rail" causing a significant decrease in the performance of the system.

In order to solve this problem a MEMS specific controller was designed that took the phase information directly from the SRI and sent it to the DM, skipping the reconstruction all together. Currently, the MEMS controller scales the phase to DM space and appropriately applies the servo gains. This is also where any piston and reference removal is calculated. Initial data with the MEMS specific controller showed marked improvement in performance over running with the conventional RTR,[4] but has also allowed the $mod(2\pi)$ nature of the MEMS DM to become evident. Here we will experimentally demonstrate this behavior and briefly discuss possible optimization methods.

3. EXPERIMENTAL SETUP

The ASALT lab is well equipped to test multiple different types of DM's under the same turbulence conditions. Our optical bench contains both a Boston MicroMachines MEMS DM as well as a Xinetics DM. Each DM uses a self referencing interferometer wavefront sensor (SRI-WFS).

3.1 Testbed

ASALT uses an Atmospheric Turbulence Simulator (ATS) to simulate a two layer atmosphere with Kolmogorov turbulence.[6] The ATS consists of two phase screens generated by LexiTek used to simulate low and high altitudes. The ATS allows for well controlled, repeatable atmospheric conditions by controlling r_0 (Fried's coherence length), Rytov number (log-amplitude variance), and Greenwood frequency (characteristic frequency of the tilt of the atmosphere).

The optical table uses a 1550nm laser as the source. This laser is propagated through the ATS which imprints a scaled version of the turbulence profile onto its phase. A fast steering mirror (FSM) compensates for the overall tip and tilt of the wavefront. The respective DM then applies a high-order correction to the wavefront. Once reflected off the DM the beam is sent to a SRI-WFS that directly measures the phase of the beam in $mod(2\pi)$ space.[7] Figure 2 shows the optical layout of the table. The two DM's are placed conjugate to the pupil and the WFS, i.e. they see the same wavefront as is in the entrance aperture (pupil) at the telescope.

3.2 MEMS Deformable Mirror

The DM used in this particular experiment is a Boston Micromachines MEMS segmented device with 1024 actuators, a pixel pitch of 300μm and a fill factor of 98%. Mechanically, the power consumption of the MEMS is approximately 40W with a volume of $0.014m^3$ and a weight of less than 5kg. This particular MEMS DM has an actuator throw of 1.5μm. Figure 3 shows the actuator scheme of a segmented and a continuous face sheet DM for comparison.

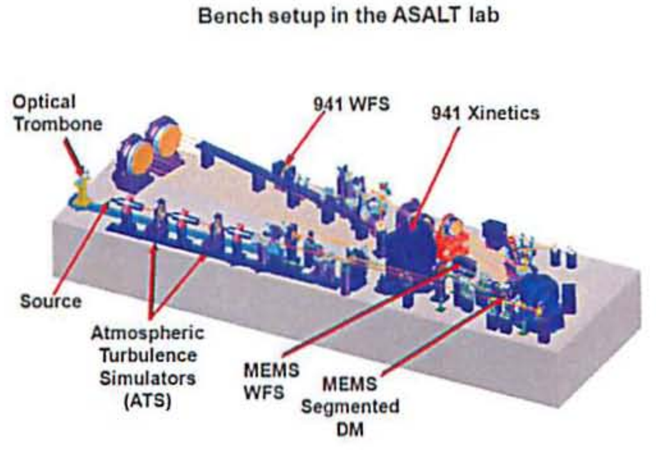

Fig. 2. *Optical layout for the table used in the ASALT lab*

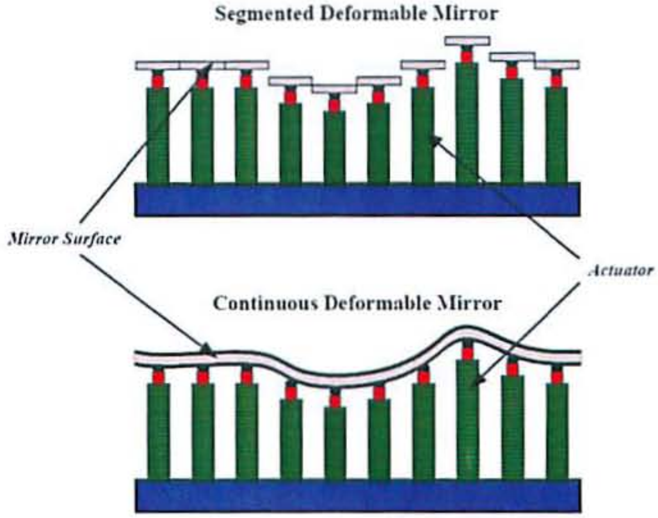

Fig. 3. *Example of two different types of deformable mirrors*.[8]

3.3 Control Interface

The control interface consists of multiple computers that interface with different pieces of hardware on the table. Separate computers control each DM, scoring camera, WFS, etc. The main console controls all of the systems. This console consists of specific modules that merge both hardware control and processing algorithms. This console is highly flexible allowing the user to specify multiple aspects of the optics table. It is here where a specific RTR is implemented, WFS reference files can be specified, phase wheel speeds can be adjusted, DM controls are set, etc. Figure 4 shows the particular layout used for this experiment. Here we have an SRI RTR, which yields phase only information from the SRI, and a MEMS specific RTR which houses the MEMS control law.

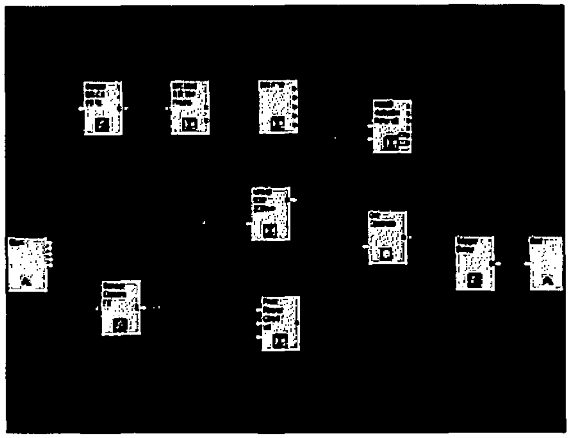

Fig. 4. *Control Interface*

4. METHODOLOGY

Implementing a MEMS specific controller has greatly improved system performance, but also has allowed the $mod(2\pi)$ nature of the MEMS DM to become apparent. With the new controller, if the phase is is such that the mirror commands the actuator to extend past its maximum throw, the actuator will "wrap around" meaning it will jump back down to try and account for the incoming phase. Generally the MEMS DM is operated in a biased mode at 50% of its stoke and the DM commands are wrapped to be in a principal domain of $[-\pi,\pi]$. Therefore if the DM commands the actuator to move $\pi+\varepsilon$ or $-\pi+\varepsilon$, the actuator will wrap around instead of railing as with the conventional RTR. When this happens the actuator has to traverse its full stroke and this added delay increases the likelihood of measuring an incorrect phase. This will cause the response of the system to degrade and introduce discontinuities in the resulting mirror commands.

The idea here is to demonstrate the mod(2π) nature of the MEMS DM, which is best achieved by analyzing the response of the system in the frequency domain. Rejection functions are frequently used to determine the response of an AO system to incoming disturbances. The disturbance is defined as the incoming aberrated phase while the response is the residual phase off the DM .[8] In our case the response of the system can be calculated using the mirror commands sent to the DM for the corresponding disturbance as a function of frequency, i.e.

$$\S(\omega) = \frac{y(\omega)}{d(\omega)}, \tag{2}$$

where $y(\omega)$ is the known mirror commands sent to the DM and $d(\omega)$ is the corresponding disturbance as a function of frequency. The error rejection curve plots the response of the system (usually in dB's) versus the frequency. In the ideal case, as the frequency is increased the response should asymptotically approach zero. Figure 5 shows an example of a theoretical error rejection curve along with the corresponding noise rejection function .[8]

We discuss two methods to show the mod(λ) nature of the MEMS DM. The first method drove a single actuator with a sinusoidal disturbance with varying frequency and amplitude. The actuator was driven from outside the control loop meaning the disturbance is placed on the mirror, rather than coming from the wavefront sensor. Figure 6 shows where the disturbance was added with respect to the controller.

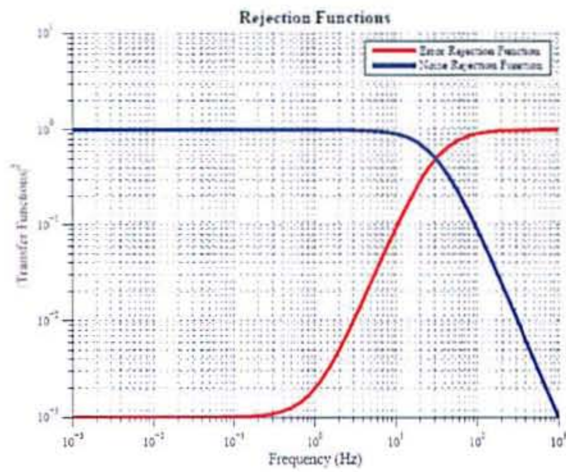

Fig. 5. *Example of a typical error rejection curve*

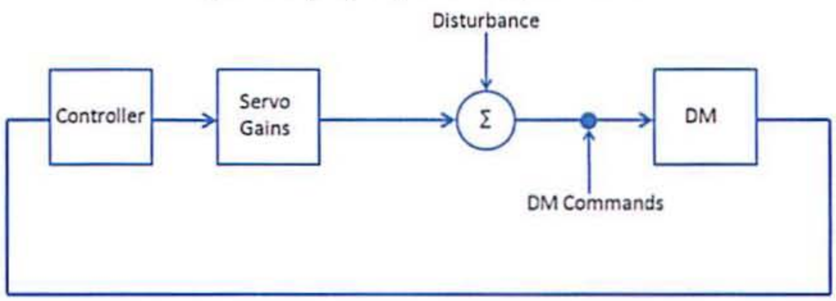

Fig. 6. *Diagram of the control law implemented for a single actuator poke.*

For this setup we also biased the piston settings on the DM. This setting adjusts the position of the actuators starting points. For our initial data runs the DM was pistoned to 50% of its range. Sending in a disturbance with low amplitude in this case will result in the actuator moving about the center of its range i.e. showing normal performance. The piston was then set at a zero bias such that the actuators all started at their minimum position allowing for the wrap around effect to be seen. At this setting the actuators are moving about the minimum and maximum range of their throw, i.e. showing $mod(2\pi)$ jumps in the mirror commands. Throughout the experiment the amplitude and frequency of the incoming disturbance was varied, along with the bias on the DM.

The second method made use of the fast steering mirror (FSM), which normally removes tilt on the wavefront. We again drove the DM with a sinusoidal disturbance, but this time generated by several waves of tilt on the FSM. In this case the disturbance was introduced before the controller, i.e. the wavefront sensor processes the disturbance as opposed to putting the disturbance directly on the DM as in the first approach. As mentioned earlier, the DM commands are "wrapped" in a principal domain of $[-\pi, \pi]$. Using the FSM to produce the disturbance allows us to see one actuator performing normally while a neighboring actuator shows the $+\pi, -\pi$ jumps. Figure 7 shows where the disturbance was added with respect to the controller.

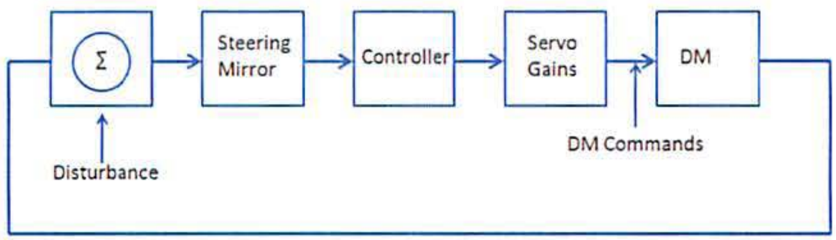

Fig. 7. *Diagram of the control law implemented for FSM method.*

5. RESULTS

As mentioned, the analysis metrics chosen for this experiment are the error rejection curves and the DM commands. Figure 8 shows an error rejection curve for the MEMS DM under normal closed loop operation driving one actuator with a sinusoidal disturbance while Figure 9 shows the corresponding mirror commands for each frequency tested. In this case the DM was biased at 50% of its throw range. The error rejection curve has the proper functional form; as the frequency increases the response should asymptotically approach zero, which is what we are seeing here. The mirror commands also show no indication of any discontinuities.

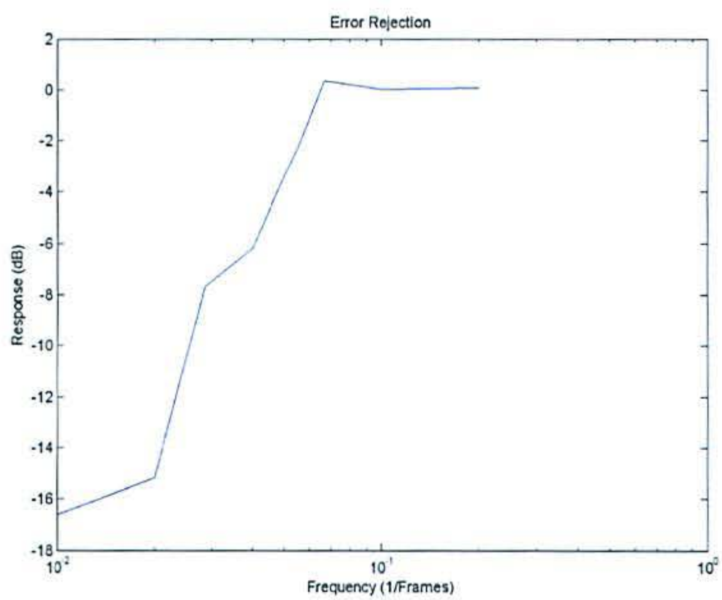

Fig. 8. *Error rejection curve.*

Figure 10 shows the error rejection curve for a data set where there was a zero bias on the DM, while Figure 11 shows the corresponding mirror commands. The error rejection curve in this case is not showing a typical response, and by looking at the corresponding DM commands it is clear why. The mirror commands are showing large discontinues indicating the actuator in question had to wrap around in order to correct for the incoming disturbance.

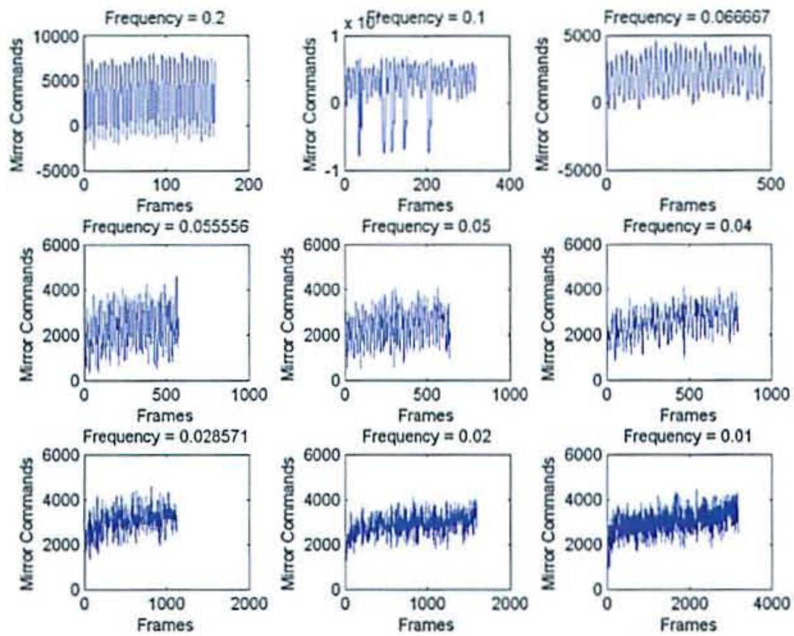

Fig. 9. *Mirror commands.*

The second method using the FSM also shows similar results. Figure 12 shows two neighboring actuators with two very different sets of mirror commands. This shows a particular actuator demonstrating the $mod(\lambda)$ effect and its neighboring actuator operating normally.

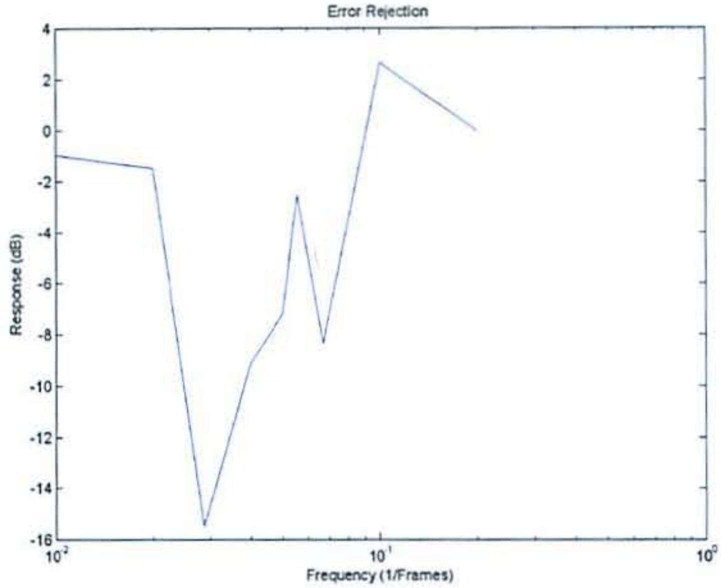

Fig. 10. *Error rejection curve demonstrating the* $mod(2\pi)$ *nature of the DM.*

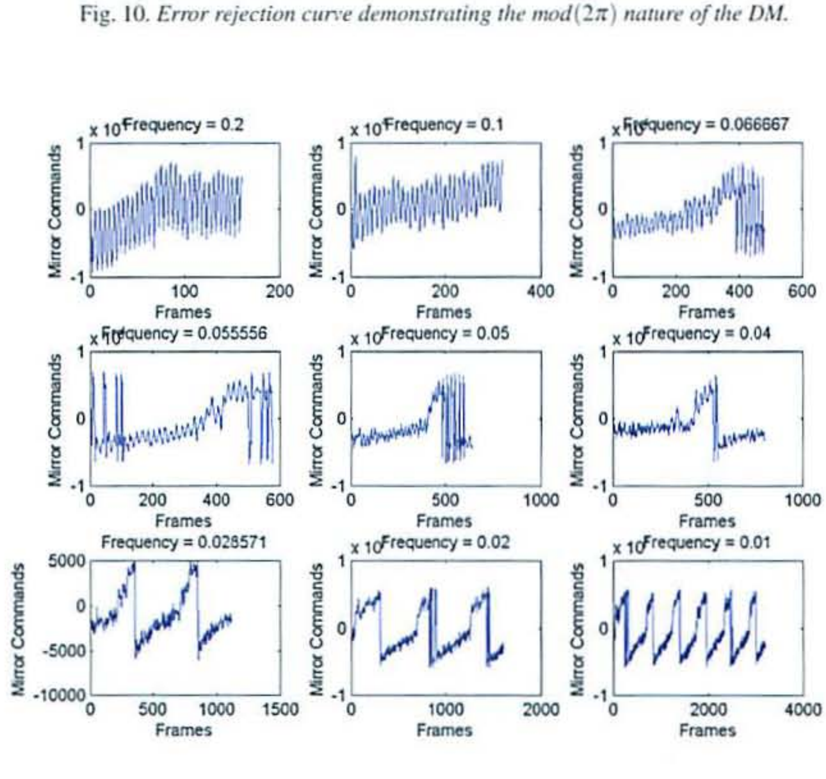

Fig. 11. *Mirror commands showing* 2π *discontinuities.*

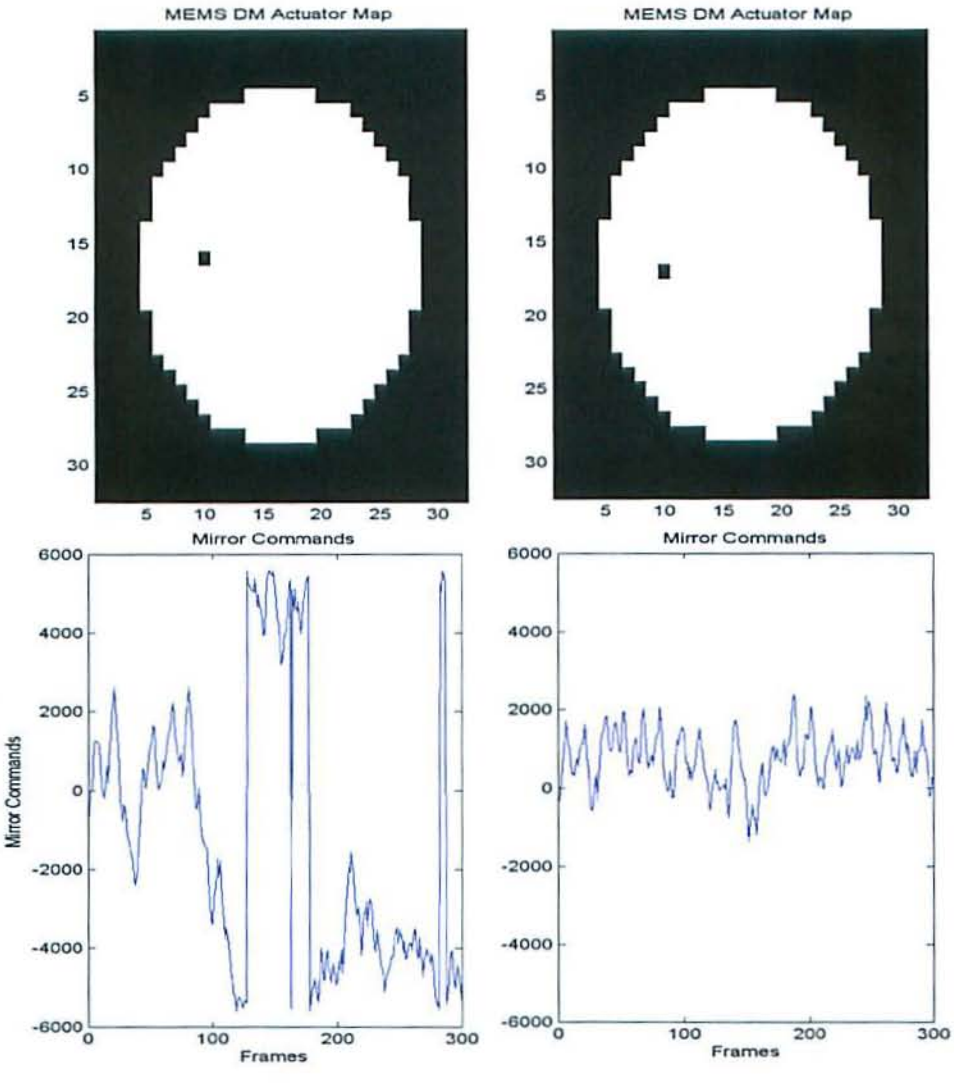

Fig. 12. *The top plots show the actuator location while the bottom plots show the corresponding mirror commands.*

6. DISCUSSION AND CONCLUSION

The goal of this research was to demonstrate the effects of a $mod(\lambda)$ DM. We successfully showed the implications of this in the error rejection curves and the corresponding mirror commands. Discussed were two separate methods used to demonstrate the issue; one by sending a sinusoidal disturbance directly to one actuator of the MEMS DM and a second method using the FSM to induce tilt on the wavefront. We have begun to address the need for an optimized MEMS specific controller, i.e. we designed an controller that can eliminate the effects of individual actuators railing, but in order to correct for the wrap around effect the current control law must be modified. This will involve looking more closely at the servo gains and how they are effecting the DM commands. It has been proposed that implementing a time varying control law will reduce the probability of individual actuators wrapping around. This will require different A and B gains for different actuators depending upon the phase at a particular time. Over the next several months we will begin to investigate new control law methods focusing on how the A and B gains are being utilized and applied.

REFERENCES

1. Robert K Tyson. *Field Guide to Adaptive Optics.* SPIE Press, 2004.
2. Robert Q. Fugate. Osa optics handout volume iii, 2000.
3. Julie C. Smith, Darryl J. Sanchez, Denis W. Oesch, Patrick R. Kelly, Carolyn M. Tewksbury-Christle, and Kevin P. Vitayaudom. Initial Results from Implementing and Testing a MEMS Adaptive Optics System. In Richard Carerras, Troy Rhoadharmer, and David Dayton, editors, *2009 SPIE Annual Conference.* SPIE, 2009.
4. Julie C. Smith, Darryl J. Sanchez, Denis W. Oesch, Carolyn M. Tewksbury-Christle, Charles C. Beckner Jr., Kevin P. Vitayaudom, Patrick R. Kelly, and Nathan E. Glauvitz. Direct Experimental Comparison between a MEMS Segmented Deformable Mirror and a Xinetics Deformable Mirror. In Daniel Herrick, editor, *2009 DEPS Annual Conference.* Directed Energy Professional Society, 2009. Published in briefing format only.
5. Julie C. Smith, Darryl J. Sanchez, Patrick R. Kelly, Denis W. Oesch, Carolyn M. Tewksbury-Christle, and Katia Shtyrkova. Experimental results demonstrating mems performance in deep turbulence. In Daniel Herrick, editor, *2010 DEPS Annual Conference.* Directed Energy Professional Society, 2010.
6. S. V. Mantravadi, T. A. Rhoadarmer, and R. S. Glas. Simple laboratory system for generating well-controlled atmospheric-like turbulence. In Michael K. Giles, John D. Gonglewshi, and Richard A. Carerras, editors, *Advanced Wavefront Control: Methods, Devices, and Applications II,* volume 5553 of *Presented at the Society of Photo-Optical Instrumentation Engineers (SPIE) Conference,* pages 290–300, Oct 2004.
7. Troy A. Rhoadarmer and Laura M. Klein. Design of a spatially phase shifted self-referencing interferometer wave front sensor. In Michael K. Giles, John D. Gonglewshi, and Richard A. Carerras, editors, *Advanced Wavefront Control: Methods, Devices, and Applications IV.* SPIE, 2006.
8. Kevin P. Vitayaudom. Analysis of Non-Uniform Gain for Control of a Deformable Mirror in an Adaptive-Optics System. Master's Thesis, AFIT/GE/ENG/08-35. School of Engineering and Management, Air Force Institute of Technology (AU), Wright-Patterson AFB OH, March 2008.

DISTRIBUTION LIST

DTIC/OCP 8725 John J. Kingman Rd, Suite 0944 Ft Belvoir, VA 22060-6218	1 cy
AFRL/RVIL Kirtland AFB, NM 87117-5776	2 cy
Patrick Kelly Official Record Copy AFRL/RDSAE	1 cy